Observation of a $J^{PC} = 1^{-+}$ Exotic Resonance in Diffractive Dissociation of 190 GeV/c π^- into $\pi^-\pi^-\pi^+$

M. G. Alekseev,[28] V. Yu. Alexakhin,[7] Yu. Alexandrov,[15] G. D. Alexeev,[7] A. Amoroso,[27] A. Austregesilo,[10,17] B. Badełek,[30] F. Balestra,[27] J. Ball,[22] J. Barth,[4] G. Baum,[1] Y. Bedfer,[22] J. Bernhard,[13] R. Bertini,[27] M. Bettinelli,[16] R. Birsa,[24] J. Bisplinghoff,[3] P. Bordalo,[12,†] F. Bradamante,[25] A. Bravar,[24] A. Bressan,[25] G. Brona,[10,30] E. Burtin,[22] M. P. Bussa,[27] A. Chapiro,[26] M. Chiosso,[27] S. U. Chung,[17] A. Cicuttin,[26] M. Colantoni,[28] M. L. Crespo,[26] S. Dalla Torre,[24] T. Dafni,[22] S. Das,[6] S. S. Dasgupta,[6] O. Yu. Denisov,[28] L. Dhara,[6] V. Diaz,[26] A. M. Dinkelbach,[17] S. V. Donskov,[21] N. Doshita,[2,22] V. Duic,[25] W. Dünnweber,[16] A. Efremov,[7] A. El Alaoui,[22] P. D. Eversheim,[3] W. Eyrich,[8] M. Faessler,[16] A. Ferrero,[27,10] M. Finger,[19] M. Finger, Jr.,[7] H. Fischer,[9] C. Franco,[12] J. M. Friedrich,[17] R. Garfagnini,[27] F. Gautheron,[2] O. P. Gavrichtchouk,[7] R. Gazda,[30] S. Gerassimov,[15,17] R. Geyer,[16] M. Giorgi,[25] B. Gobbo,[24] S. Goertz,[2,4] S. Grabmüller,[17] O. A. Grajek,[30] A. Grasso,[27] B. Grube,[17] R. Gushterski,[7] A. Guskov,[7] F. Haas,[17] D. von Harrach,[13] T. Hasegawa,[14] J. Heckmann,[2] F. H. Heinsius,[9] R. Hermann,[13] F. Herrmann,[9] C. Heß,[2] F. Hinterberger,[3] N. Horikawa,[18,§] Ch. Höppner,[17] N. d'Hose,[22] C. Ilgner,[10,16] S. Ishimoto,[18,¶] O. Ivanov,[7] Yu. Ivanshin,[7] T. Iwata,[32] R. Jahn,[3] P. Jasinski,[13] G. Jegou,[22] R. Joosten,[3] E. Kabuß,[13] D. Kang,[9] B. Ketzer,[17] G. V. Khaustov,[21] Yu. A. Khokhlov,[21] Yu. Kisselev,[2] F. Klein,[4] K. Klimaszewski,[30] S. Koblitz,[13] J. H. Koivuniemi,[2] V. N. Kolosov,[21] E. V. Komissarov,[7,*] K. Kondo,[2,32] K. Königsmann,[9] R. Konopka,[17] I. Konorov,[15,17] V. F. Konstantinov,[21] A. Korzenev,[13,‡] A. M. Kotzinian,[7,22] O. Kouznetsov,[7,22] K. Kowalik,[30,22] M. Krämer,[17] A. Kral,[20] Z. V. Kroumchtein,[7] R. Kuhn,[17] F. Kunne,[22] K. Kurek,[30] L. Lauser,[9] J. M. Le Goff,[22] A. A. Lednev,[21] A. Lehmann,[8] S. Levorato,[25] J. Lichtenstadt,[23] T. Liska,[20] A. Maggiora,[28] M. Maggiora,[27] A. Magnon,[22] G. K. Mallot,[10] A. Mann,[17] C. Marchand,[22] J. Marroncle,[22] A. Martin,[25] J. Marzec,[31] F. Massmann,[3] T. Matsuda,[14] A. N. Maximov,[7,*] W. Meyer,[2] T. Michigami,[32] Yu. V. Mikhailov,[21] M. A. Moinester,[23] A. Mutter,[9,13] A. Nagaytsev,[7] T. Nagel,[17] J. Nassalski,[30,*] T. Negrini,[3] F. Nerling,[9] S. Neubert,[17] D. Neyret,[22] V. I. Nikolaenko,[21] A. G. Olshevsky,[7] M. Ostrick,[13] A. Padee,[31] R. Panknin,[4] D. Panzieri,[29] B. Parsamyan,[27] S. Paul,[17] B. Pawlukiewicz-Kaminska,[30] E. Perevalova,[7] G. Pesaro,[25] D. V. Peshekhonov,[7] G. Piragino,[27] S. Platchkov,[22] J. Pochodzalla,[13] J. Polak,[11,25] V. A. Polyakov,[21] G. Pontecorvo,[7] J. Pretz,[4] C. Quintans,[12] J.-F. Rajotte,[16] S. Ramos,[12,†] V. Rapatsky,[7] G. Reicherz,[2] D. Reggiani,[10] A. Richter,[8] F. Robinet,[22] E. Rocco,[27] E. Rondio,[30] D. I. Ryabchikov,[21] V. D. Samoylenko,[21] A. Sandacz,[30] H. Santos,[12] M. G. Sapozhnikov,[7] S. Sarkar,[6] I. A. Savin,[7] G. Sbrizzai,[25] P. Schiavon,[25] C. Schill,[9] T. Schlüter,[16] L. Schmitt,[17,‖] S. Schopferer,[9] W. Schröder,[8] O. Yu. Shevchenko,[7] H.-W. Siebert,[13] L. Silva,[12] L. Sinha,[6] A. N. Sissakian,[7] M. Slunecka,[7] G. I. Smirnov,[7] S. Sosio,[27] F. Sozzi,[25] A. Srnka,[5] M. Stolarski,[30,10] M. Sulc,[11] R. Sulej,[31] S. Takekawa,[25] S. Tessaro,[24] F. Tessarotto,[24] A. Teufel,[8] L. G. Tkatchev,[7] S. Uhl,[17] I. Uman,[16] G. Venugopal,[3] M. Virius,[20] N. V. Vlassov,[7] A. Vossen,[9] Q. Weitzel,[17] R. Windmolders,[4] W. Wiślicki,[30] H. Wollny,[9] K. Zaremba,[31] M. Zavertyaev,[15] E. Zemlyanichkina,[7] M. Ziembicki,[31] J. Zhao,[13,24] N. Zhuravlev,[7] and A. Zvyagin[16]

(COMPASS Collaboration)

[1]*Universität Bielefeld, Fakultät für Physik, 33501 Bielefeld, Germany*
[2]*Universität Bochum, Institut für Experimentalphysik, 44780 Bochum, Germany*
[3]*Universität Bonn, Helmholtz-Institut für Strahlen- und Kernphysik, 53115 Bonn, Germany*
[4]*Universität Bonn, Physikalisches Institut, 53115 Bonn, Germany*
[5]*Institute of Scientific Instruments, AS CR, 61264 Brno, Czech Republic*
[6]*Matrivani Institute of Experimental Research & Education, Calcutta-700 030, India*
[7]*Joint Institute for Nuclear Research, 141980 Dubna, Moscow region, Russia*
[8]*Universität Erlangen-Nürnberg, Physikalisches Institut, 91054 Erlangen, Germany*
[9]*Universität Freiburg, Physikalisches Institut, 79104 Freiburg, Germany*
[10]*CERN, 1211 Geneva 23, Switzerland*
[11]*Technical University in Liberec, 46117 Liberec, Czech Republic*
[12]*LIP, 1000-149 Lisbon, Portugal*
[13]*Universität Mainz, Institut für Kernphysik, 55099 Mainz, Germany*
[14]*University of Miyazaki, Miyazaki 889-2192, Japan*
[15]*Lebedev Physical Institute, 119991 Moscow, Russia*
[16]*Ludwig-Maximilians-Universität München, Department für Physik, 80799 Munich, Germany*
[17]*Technische Universität München, Physik Department, 85748 Garching, Germany*
[18]*Nagoya University, 464 Nagoya, Japan*

[19]Charles University in Prague, Faculty of Mathematics and Physics, 18000 Prague, Czech Republic
[20]Czech Technical University in Prague, 16636 Prague, Czech Republic
[21]State Research Center of the Russian Federation, Institute for High Energy Physics, 142281 Protvino, Russia
[22]CEA IRFU/SPhN Saclay, 91191 Gif-sur-Yvette, France
[23]Tel Aviv University, School of Physics and Astronomy, 69978 Tel Aviv, Israel
[24]Trieste Section of INFN, 34127 Trieste, Italy
[25]University of Trieste, Department of Physics and Trieste Section of INFN, 34127 Trieste, Italy
[26]Abdus Salam ICTP and Trieste Section of INFN, 34127 Trieste, Italy
[27]University of Turin, Department of Physics and Torino Section of INFN, 10125 Turin, Italy
[28]Torino Section of INFN, 10125 Turin, Italy
[29]University of Eastern Piedmont, 1500 Alessandria, and Torino Section of INFN, 10125 Turin, Italy
[30]Soltan Institute for Nuclear Studies and University of Warsaw, 00-681 Warsaw, Poland
[31]Warsaw University of Technology, Institute of Radioelectronics, 00-665 Warsaw, Poland
[32]Yamagata University, Yamagata, 992-8510 Japan

(Received 12 November 2009; published 18 June 2010)

The COMPASS experiment at the CERN SPS has studied the diffractive dissociation of negative pions into the $\pi^-\pi^-\pi^+$ final state using a 190 GeV/c pion beam hitting a lead target. A partial wave analysis has been performed on a sample of 420 000 events taken at values of the squared 4-momentum transfer t' between 0.1 and 1 GeV$^2/c^2$. The well-known resonances $a_1(1260)$, $a_2(1320)$, and $\pi_2(1670)$ are clearly observed. In addition, the data show a significant natural-parity exchange production of a resonance with spin-exotic quantum numbers $J^{PC} = 1^{-+}$ at 1.66 GeV/c^2 decaying to $\rho\pi$. The resonant nature of this wave is evident from the mass-dependent phase differences to the $J^{PC} = 2^{-+}$ and 1^{++} waves. From a mass-dependent fit a resonance mass of $(1660 \pm 10^{+0}_{-64})$ MeV/c^2 and a width of $(269 \pm 21^{+42}_{-64})$ MeV/c^2 are deduced, with an intensity of $(1.7 \pm 0.2)\%$ of the total intensity.

DOI: 10.1103/PhysRevLett.104.241803 PACS numbers: 12.39.Mk, 13.25.Jx, 14.40.Be, 14.40.Rt

In the $SU(3)_{flavor}$ constituent quark model, light mesons are described as bound states of a quark q and an antiquark $\bar{q}'$ with quark flavors u, d, s. Mesons are classified in J^{PC} multiplets, with the total angular momentum J, the parity P, and the particle-antiparticle conjugation parity C, which is defined through the neutral flavorless members of a given multiplet. The isospin I and the G parity further characterize mesons containing light quarks. In the quark model, P, C, and G are given by

$$P = (-1)^{L+1}, \qquad C = (-1)^{L+S}, \qquad G = (-1)^{I+L+S}, \tag{1}$$

where L is the relative orbital angular momentum of q and $\bar{q}'$, and S is the total intrinsic spin of the $q\bar{q}'$ pair, with $S = 0, 1$. The constituent quark model has been quite successful in explaining many of the properties of mesons as well as, to a large extent, the observed meson spectrum, even though it makes no assumptions concerning the nature of the binding force, except that hadrons are postulated to be color-singlet states. In quantum chromodynamics (QCD), the interaction between colored quarks is described by the exchange of gluons which carry color themselves. Owing to this particular structure of QCD, color-singlet mesons can be formed not only by constituent quarks, but also by other configurations like four-quark objects or gluonic excitations. These non-$q\bar{q}'$ configurations, however, will mix with ordinary $q\bar{q}'$ states with the same J^{PC}, making it difficult to disentangle the contribution of each configuration. The observation of exotic states with quantum numbers not allowed in the simple quark model, e.g., $J^{PC} = 0^{--}$, 0^{+-}, 1^{-+}, ..., would give clear evidence that quark-gluon configurations beyond the quark model, as allowed by QCD, are realized in nature.

The lowest-lying hybrid, i.e., a system consisting of a color octet $q\bar{q}'$ pair neutralized in color by a gluonic excitation, is expected [1] to have exotic quantum numbers $J^{PC} = 1^{-+}$, and thus will not mix with ordinary mesons. Its mass is predicted in the region 1.3–2.2 GeV/c^2. The systematics of hybrid meson production and decay has been worked out in the flux-tube model [2]. There are three experimental candidates for a light 1^{-+} hybrid. The $\pi_1(1400)$ was observed by the E852 (BNL, U.S.) [3] and VES (Protvino, Russia) [4] experiments in the reaction $\pi^- N \to \eta\pi^- N$, and by the Crystal Barrel experiment [5,6] in $\bar{p}n \to \pi^-\pi^0\eta$ and $\bar{p}p \to 2\pi^0\eta$ Dalitz plot analyses. Another 1^{-+} state, the $\pi_1(1600)$, decaying into $\rho\pi$ [7–9], $\eta'\pi$ [10,11], $f_1(1285)\pi$ [12,13], and $b_1(1235)\pi$ [13,14] was observed in peripheral $\pi^- p$ interactions in E852 and VES, and confirmed in $\bar{p}p \to b_1(1235)\pi\pi$ [15]. The resonant nature of both states, however, is still heavily disputed in the community [4,13]. In a different analysis of a larger data set of E852 no evidence for an exotic resonance at 1.6 GeV/c^2 in the 3π final state was found [16]. A third exotic state, $\pi_1(2000)$, decaying to $f_1(1285)\pi$ and $b_1(1235)\pi$, was seen in only one experiment [12,14].

In order to shed new light on these questions, the COMPASS Collaboration, operating a large-acceptance and high-resolution spectrometer [17] situated at the CERN Super Proton Synchrotron (SPS), is gathering high-statistics event samples of diffractive reactions of hadronic probes into final states containing both charged and neutral particles. Diffractive dissociation is a reaction of the type $a + b \to c + d$ with $c \to 1 + 2 + \cdots + n$, where a is the incoming beam particle, b the target, c the diffractively produced object decaying into n particles, and d the target recoil particle, with 4-momenta $p_a \ldots p_d$, respectively. The production kinematics is described by two variables: s and $t' = |t| - |t|_{\min}$, where $s = (p_a + p_b)^2$ is the square of the total center of mass energy, $t = (p_a - p_c)^2$ is the square of the four momentum transferred from the incoming beam to the outgoing system c, and $|t|_{\min}$ is the minimum value of $|t|$ which is allowed by kinematics for a given mass m_c.

First studies of diffractive reactions of 190 GeV/c π^- on a 3 mm lead target were carried out by COMPASS in 2004. The $\pi^-\pi^-\pi^+$ final state was chosen because the disputed $\pi_1(1600)$ meson with exotic J^{PC} had previously been reported in this channel. The trigger selected events with one incoming particle and at least two outgoing charged particles. In the offline analysis, a primary vertex inside the target with 3 outgoing charged particles is required. Since the recoil particle was not detected, the following procedure is applied in order to select exclusive events. The beam energy E_a is very well approximated by the measured total energy E_c of the 3π system with a small correction arising from the target recoil, which can be calculated from the measured scattering angle $\theta = \angle(\vec{p}_a, \vec{p}_c)$, assuming that the target particle remained intact throughout the scattering process. Then an exclusivity cut is applied, requiring E_a to be within ± 4 GeV of the mean beam energy. Events with a wide range of t' from zero up to a few GeV$^2/c^2$ were recorded. For the analysis presented in this letter we restrict ourselves to the range where candidates for spin-exotic states have been reported in the past: 0.1 GeV$^2/c^2 < t' < 1.0$ GeV$^2/c^2$, far beyond the region of coherent scattering on the Pb nucleus. Figure 1 shows the invariant mass of the corresponding events. In our sample of 420 000 events in the mass range between 0.5 and 2.5 GeV/c^2, the well-known resonances $a_1(1260)$, $a_2(1320)$, and $\pi_2(1670)$ are clearly visible in the 3π mass spectrum.

A partial wave analysis (PWA) of this data set was performed using a program which was originally developed at Illinois [18], and later modified at Protvino and Munich. An independent cross-check of the results was performed using a different PWA program developed at Brookhaven [19] and adapted for COMPASS [20]. At high $\sqrt{s}$, the reaction can be assumed to proceed via t-channel Reggeon exchange, thus justifying the factorization of the total cross section into a resonance and a recoil vertex

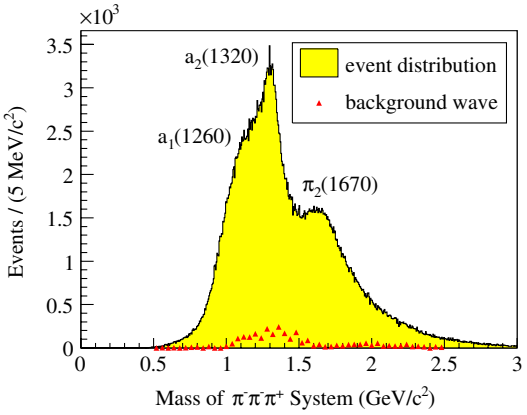

FIG. 1 (color online). Invariant mass of the 3π system for 0.1 GeV$^2/c^2 < t' < 1.0$ GeV$^2/c^2$ (histogram), and intensity of the background wave with a flat distribution in three-body phase space (triangles), obtained from a partial wave analysis in 40 MeV/c^2 bins of the 3π mass and rescaled to the binning of the histogram. Both the invariant mass spectrum and the background distribution are not acceptance corrected.

without final state interaction. The exchanged Reggeon may excite the incident pion ($J^P = 0^-$) to a state X with different J^P, limited only by conservation laws for strong interactions. For the $(3\pi)^-$ final state $I \geq 1$; we assume $I = 1$ since no flavor-exotic mesons have been found. Since in addition $G = -1$ for a system with an odd number of pions, $C = +1$ follows from Eq. (1). We take the phenomenological approach of the isobar model, in which all multiparticle final states can be described by sequential two-body decays into intermediate resonances (isobars), which eventually decay into the final state observed in the experiment. All known isovector and isoscalar $\pi\pi$ resonances have been included in our fit: $(\pi\pi)_S$ [comprising the broad $\sigma(600)$ and $f_0(1370)$], $\rho(770)$, $f_0(980)$, $f_2(1270)$, and $\rho_3(1690)$ [8]. It is possible that there exists a direct three-body decay into $(3\pi)^-$ without an intermediate di-pion resonance; in the isobar model, such a decay mode without angular correlations is represented by $\sigma(600) + \pi^-$ with $L = 0$ and $J^P = 0^-$. Possible complications to the isobar model from unitarity constraints are not an issue here; such effects enter in the formulation of the model only when all possible decay modes are simultaneously fit, which may include the final states containing π^0, η, η', ω, $K\bar{K}$, or $N\bar{N}$. The spin-parity composition of the excited state X is studied in the Gottfried-Jackson frame, which is the center of mass frame of X with the z axis along the beam direction, and the y axis perpendicular to the production plane, formed by the momentum vectors of the target and the recoil particle.

The PWA is done in two steps. In the first step, a fit of the probability density in 3π phase space is performed in 40 MeV/c^2 bins of the 3π invariant mass m (fit in mass bins). No dependence of the production strength for a given wave on the mass of the 3π system is introduced at this

point:

$$\sigma_{\text{indep}}(\tau, m, t') = \sum_{\epsilon=\pm 1} \sum_{r=1}^{N_r} \left| \sum_i T_{ir}^{\epsilon} f_i^{\epsilon}(t') \psi_i^{\epsilon}(\tau, m)/N_i^{\epsilon}(m) \right|^2,$$

$$N_i^{\epsilon}(m) = \sqrt{\int |\psi_i^{\epsilon}(\tau', m)|^2 d\tau'}. \quad (2)$$

Here, T_{ir}^{ϵ} are the production amplitudes and ψ_i^{ϵ} the decay amplitudes, the indices i and ϵ denoting different partial waves, characterized by a set of quantum numbers $J^{\text{PC}} M^{\epsilon}[\text{isobar}]L$; M is the absolute value of the spin projection onto the z axis; ϵ is the reflectivity [21], which describes the symmetry under a reflection through the production plane, and which is defined such that it corresponds to the naturality of the exchanged Regge trajectory; L is the orbital angular momentum between the isobar and the bachelor pion. The different t' dependence of the cross section for $M = 0$ and $M = 1$ states is taken into account by including different functions of t', $f_i^{\epsilon}(t') \propto \exp(-bt')$ $(M = 0)$, and $f_i^{\epsilon}(t') \propto t' \exp(-bt')$ $(M = 1)$, where the slope b has been obtained from the data by first making fits in slices of t'. The three-body decay amplitudes ψ_i^{ϵ} are constructed using nonrelativistic Zemach tensors [22]. They are properly Bose symmetrized to take into account the combinatorics due to the spin-0 nature of the final state pions. They depend on the set of five parameters τ specifying the three-body decay kinematics, but do not contain any free parameters. The normalization factors $N_i^{\epsilon}(m)$ contain angular-momentum barrier factors and quasi-two-body phase-space factors, taking into account the nonzero widths of isobars. Dividing each decay amplitude by $N_i^{\epsilon}(m)$ compensates its dependence on the mass inside each mass bin. Equation (2) includes a coherent sum over waves with different $J^{\text{PC}} M$, allowing them to interfere. It also contains two noncoherent sums over the reflectivity ϵ and the rank N_r [21]. Assuming that the recoiling target particle is a nucleon, and neglecting nuclear effects, we set $N_r = 2$, corresponding to a mixture of helicity-flip and helicity-non-flip processes at the baryon vertex. A total of 42 partial waves are included in the first step of the fit. It comprises the nonexotic positive-reflectivity waves with $J^{\text{PC}} = 0^{-+}$ $(M = 0)$, 1^{++}, 2^{-+}, 3^{++}, 4^{-+} $(M = 0,\ 1)$, 2^{++}, 4^{++} $(M = 1)$, the exotic 1^{-+} $(M = 1)$, and the negative-reflectivity waves 1^{-+}, 2^{++} $(M = 0,\ 1)$, 1^{++}, 2^{-+} $(M = 1)$, taking into account all relevant known decay modes into the isobars listed above. The fit also contains a background wave, characterized by a uniform distribution in three-body phase space, which is added incoherently to the other waves. In the fit the elements of the spin-density matrix, given by $\rho_{ij}^{\epsilon} = \sum_r T_{ir}^{\epsilon} T_{jr}^{\epsilon *}$, are determined simultaneously for all 42 waves in a given mass bin using an extended maximum likelihood method. The diagonal elements of the spin-density matrix are the intensities of the corresponding waves, while the off-diagonal elements determine the phase differences between two waves. There is no *a priori* assumption on a resonant behavior of a given wave at this first step. The fit also takes into account the experimental acceptance of the spectrometer, calculated from a phase-space Monte Carlo simulation of the apparatus. It is worth stressing that COMPASS has an excellently uniform acceptance for diffractively produced 3π events of the order of 60% over the whole phase space. In order to verify that indeed the global maximum has been found by the fit, up to 100 attempts with randomly chosen start parameters are performed for each mass bin. If multiple solutions are found within one unit of log-likelihood, the average of the two extreme solutions for each parameter is used. The difference of the two extreme solutions is added linearly to the statistical error of the best fit for each parameter.

In the second step of the PWA a χ^2 fit of the spin-density matrix elements obtained for each mass bin in the first step is performed in the mass range from 0.8 to 2.32 GeV/c^2, taking into account the mass dependence of the produced resonances (mass-dependent fit). The elements of the spin-density matrix are expressed as $\rho_{ij}^{\epsilon} = \sum_r A_{ir}^{\epsilon}(m) A_{jr}^{\epsilon *}(m)$ with amplitudes $A_{ir}^{\epsilon}(m) = \sum_k C_{ikr}^{\epsilon} \text{BW}_k(m) N_i^{\epsilon}(m)$, with $\text{BW}_k(m)$ denoting relativistic Breit-Wigner functions (with constant or dynamic widths depending on whether branching ratios of the corresponding resonance are known) or, where required by the fit, a coherent background reflecting nonresonant production of the corresponding partial wave, e.g., via the Deck effect [23]. For the latter, an empirical parametrization consisting of a simple exponential, $\exp(-\alpha p^2)$, with p being the breakup momentum for the two-body decay of the produced resonance and α a fit parameter, is used. In the mass-dependent fit the complex production amplitudes C_{ikr}^{ϵ}, and the parameters of $\text{BW}_k(m)$ are determined for a subset of six waves, the selected waves showing either significant amplitudes or rapid relative phase changes in the 1.7 GeV/c^2 mass range: $0^{-+}0^+ f_0(980)\pi S$, $1^{++}0^+ \rho\pi S$, $2^{-+}0^+ f_2\pi S$, $2^{++}1^+ \rho\pi D$, $4^{++}1^+ \rho\pi G$, and the exotic $1^{-+}1^+ \rho\pi P$.

The intensity of the background wave resulting from the fit in mass bins is included in Fig. 1 (triangles). Figures 2(a)–2(c) show the acceptance-corrected intensities of the three most prominent waves $1^{++}0^+ \rho\pi S$, $2^{-+}0^+ f_2\pi S$, and $2^{++}1^+ \rho\pi D$, respectively, as determined from the fit in mass bins (data points with error bars). The data also show a significant natural-parity exchange production of a wave with spin-exotic quantum numbers $J^{\text{PC}} = 1^{-+}$ at 1.66 GeV/c^2 decaying to $\rho\pi$ (P wave), presented in Fig. 2(d). The resonant nature of the exotic wave is evident from its phase differences to the dominant $1^{++}0^+ \rho\pi S$ and $2^{-+}0^+ f_2\pi S$ waves, shown in Figs. 3(a) and 3(b), respectively (data points). For the latter, shown in Fig. 3(b), no significant change in the phase difference between 1.4 and 1.9 GeV/c^2 is observed, which is attributed to the fact that there are two resonances, $\pi_1(1600)$ and

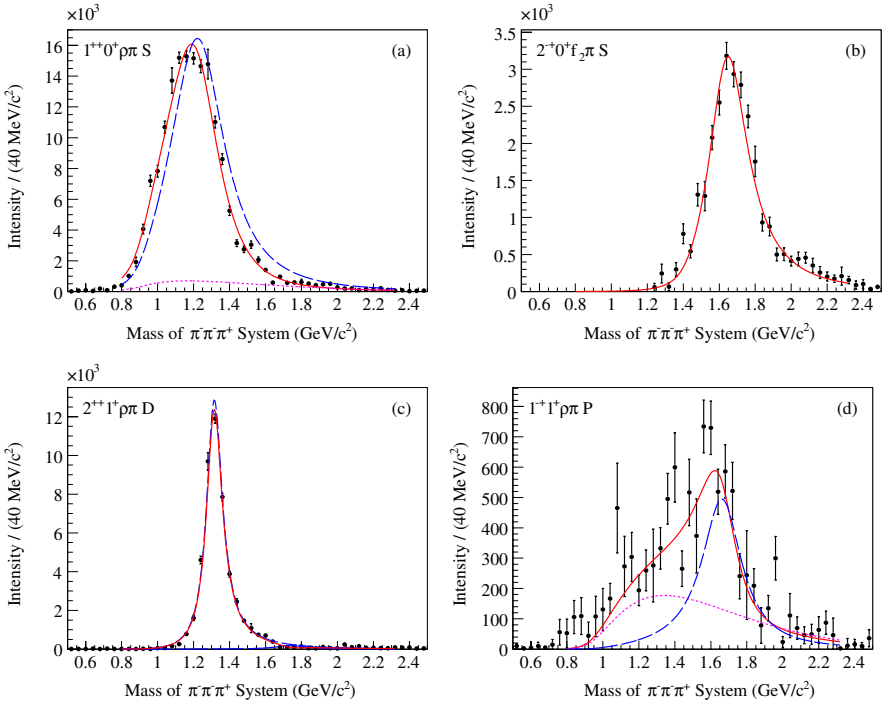

FIG. 2 (color online). Intensities of major waves $1^{++}0^{+}\rho\pi S$ (a), $2^{-+}0^{+}f_2\pi S$ (b), and $2^{++}1^{+}\rho\pi D$ (c), as well as the intensity of the exotic wave $1^{-+}1^{+}\rho\pi P$ (d), as determined in the fit in mass bins (data points with error bars). The lines represent the result of the mass-dependent fit (see text).

$\pi_2(1670)$, with very similar masses and widths, causing the relative phase difference to be almost constant. In contrast to this the phase difference to the 1^{++} wave, shown in Fig. 3(a), clearly shows an increase around 1.7 GeV/c^2. As the $a_1(1260)$ is no longer resonating at this mass, this observation can be regarded as an independent verification of the resonating nature of the 1^{-+} wave.

The solid lines in Fig. 2 show the total intensity from the mass-dependent fit for the corresponding waves. For the $1^{++}0^{+}\rho\pi S$ wave shown in Fig. 2(a) it is well known that there is a significant contribution of nonresonant production through the Deck effect [24], indicated by the dotted line. Its interference with the $a_1(1260)$ (dashed line) shifts the peak in the data to a slightly lower value than the peak position of the resonance. The $2^{-+}0^{+}f_2\pi S$ wave shown in Fig. 2(b) is well described by a single resonance, the $\pi_2(1670)$. The $2^{++}1^{+}\rho\pi D$ wave displayed in Fig. 2(c) is dominated by the $a_2(1320)$ with a small contribution from the $a_2(1700)$, whose parameters have been fixed to Particle Data Group (PDG) values [25] because of the limited statistics. The intensity of the exotic $1^{-+}1^{+}\rho\pi P$ wave, shown in Fig. 2(d), is well described by a Breit-Wigner resonance with constant width at 1.66 GeV/c^2 (dashed line), which we interpret as the $\pi_1(1600)$, and a nonresonant background (dotted line) at lower masses. The resonant component of the exotic wave is strongly constrained by the mass-dependent phase differences to the $1^{++}0^{+}\rho\pi S$ and the $2^{-+}0^{+}f_2\pi S$ waves, which are well

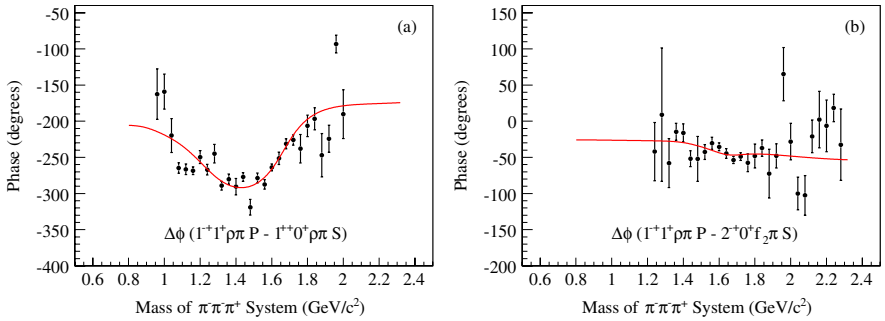

FIG. 3 (color online). Phase differences of the exotic $1^{-+}1^{+}\rho\pi P$ wave to the $1^{++}0^{+}\rho\pi S$ (a) and the $2^{-+}0^{+}f_2\pi S$ (b) waves. The data points represent the result of the fit in mass bins; the lines are the result of the mass-dependent fit.

TABLE I. Resonance masses, total widths, and intensities for the specified decay channel of the six waves included in the mass-dependent fit to the data. The first uncertainty corresponds to the statistical error, the asymmetric second one to the systematic error. The last two columns give the corresponding PDG values [26].

Resonance	Mass (MeV/c^2)	Width (MeV/c^2)	Intensity (%)	Channel $J^{PC}M^{\epsilon}$[isobar]L	Mass [26] (MeV/c^2)	Width [26] (MeV/c^2)
$a_1(1260)$	$1255 \pm 6^{+7}_{-17}$	$367 \pm 9^{+28}_{-25}$	$67 \pm 3^{+4}_{-20}$	$1^{++}0^{+}\rho\pi S$	1230 ± 40	250–600
$a_2(1320)$	$1321 \pm 1^{+0}_{-7}$	$110 \pm 2^{+2}_{-15}$	$19.2 \pm 0.6^{+0.3}_{-2.2}$	$2^{++}1^{+}\rho\pi D$	1318.3 ± 0.6	107 ± 5
$\pi_1(1600)$	$1660 \pm 10^{+0}_{-64}$	$269 \pm 21^{+42}_{-64}$	$1.7 \pm 0.2^{+0.9}_{-0.1}$	$1^{-+}1^{+}\rho\pi P$	1662^{+15}_{-11}	234 ± 50
$\pi_2(1670)$	$1658 \pm 3^{+24}_{-8}$	$271 \pm 9^{+22}_{-24}$	$10.0 \pm 0.4^{+0.7}_{-0.7}$	$2^{-+}0^{+}f_2\pi S$	1672.4 ± 3.2	259 ± 9
$\pi(1800)$	$1785 \pm 9^{+12}_{-6}$	$208 \pm 22^{+21}_{-37}$	$0.8 \pm 0.1^{+0.3}_{-0.1}$	$0^{-+}0^{+}f_0\pi S$	1816 ± 14	208 ± 12
$a_4(2040)$	$1885 \pm 13^{+50}_{-2}$	$294 \pm 25^{+46}_{-19}$	$1.0 \pm 0.3^{+0.1}_{-0.1}$	$4^{++}1^{+}\rho\pi G$	2001 ± 10	313 ± 31

reproduced in the mass-dependent fit (solid lines in Fig. 3). The parameters deduced for the masses, widths, and intensities of the resonances included in the mass-dependent fit are given in Table I, where the first uncertainty corresponds to the statistical error, the second to the systematic error. The intensities are given for the resonant part of the corresponding wave integrated over the mass range from 0.8 to 2.32 GeV/c^2, and are normalized to the total intensity from the mass-dependent fit, corresponding to 38.7 (2)% of the acceptance-corrected data sample in the same mass range. The intensity of the $\pi_1(1600)$ is found to be $(1.7 \pm 0.2)\%$ of the total intensity, while the nonresonant contribution is $(1.5 \pm 0.2)\%$, with a linear correlation coefficient between the two intensities of 15%. The dominance of natural- over unnatural-parity exchange is more pronounced than in the BNL case at 18 GeV/c [8]. This is possibly due to the decreasing contribution of unnatural-parity exchange with an increasing beam energy, if the natural-parity exchange is mediated mostly by the Pomeron.

The systematic errors were estimated from the data by testing the stability of the result with respect to various assumptions made in the analysis, e.g., adding or removing certain waves, varying cuts or initial parameters for the fit. One such study concerns the choice of the rank N_r used in the PWA. Although $N_r = 2$ is physically motivated from the fact that, at high t', incoherent diffraction from individual nucleons dominates the reaction, fits with $N_r = 1$ and 3 were tried as well. The intensity in the background wave relative to the total acceptance-corrected data sample in the mass range from 0.5 to 2.5 GeV/c^2 increases from 5.8% for $N_r = 2$ to 19% for $N_r = 1$, while it drops to 1.2% for $N_r = 3$. At the same time, however, $N_r = 3$ was found to cause larger bin-to-bin fluctuations without significantly altering the result. Given the level of the present statistics, we therefore conclude that the optimum rank is $N_r = 2$. In an attempt to account for the low-mass shoulder in the intensity of the $1^{-+}1^{+}\rho\pi P$ wave we also tried to include a $\pi_1(1400)$ into the mass-dependent fit, with parameters fixed to PDG values [25]. This reduced the background intensity to a negligible value and shifted the resonance mass of the $\pi_1(1600)$ to a slightly smaller value, which is reflected in its systematic error, but did not affect the intensity or the phase differences of any of the other waves in the mass-dependent fit. Releasing the parameters of the $\pi_1(1400)$, however, causes the fit to become unstable. This can be attributed to the fact that the $\pi_1(1400)$, if present at all, couples only weakly to the $\pi^-\pi^-\pi^+$ final state. Another study of the sensitivity of the $\pi_1(1600)$ intensity to the functional form of the background was performed using a background parametrization without angular-momentum barrier factors, which did not alter the result. Other systematic studies included a shift of the 40 MeV/c^2 mass bins by 20 MeV/c^2, the use of rotation functions with relativistic factors [27] instead of Zemach tensors for the fit in mass bins, and the inclusion of four waves with $M = 2$. The use of different parametrizations for the σ and ρ mesons also did not influence the result. Performing the fit in mass bins on nonexclusive events, i.e., events outside the aforementioned exclusivity cut, no signal is observed in the 1^{-+} wave.

An incomplete acceptance of the spectrometer, not properly taken into account in the Monte Carlo simulation, or an incomplete set of waves may introduce leakage of nonexotic waves into the 1^{-+} wave. In order to study this effect, Monte Carlo events were generated using the parameters of 16 dominant waves, excluding the 1^{-+}, which were determined in a mass-dependent fit, and simulating the decay patterns of the corresponding decay channels. Performing the same PWA for the Monte Carlo data as for the real data it was found that the fraction of ''fake'' intensity in the observed 1^{-+} wave in the Monte Carlo case is less than 5%, and thus negligible.

In order to test the significance of the exotic wave, a second fit in mass bins was performed excluding the exotic wave from the wave set. A likelihood ratio test yields a log-likelihood difference of 47.3 between the two fits, averaged over a mass range of twice the experimental width around the resonance mass of the $\pi_1(1600)$. For a difference in the numbers of degrees of freedom of 4 this confirms the presence of the exotic wave in the wave set with a probability very close to unity.

In conclusion, a partial wave analysis of COMPASS data from the diffractive dissociation of 190 GeV/c π^- on a Pb target into the $\pi^-\pi^-\pi^+$ final state at 0.1 GeV$^2/c^2 < t' <$ 1.0 GeV$^2/c^2$ was performed. In addition to well-known $q\bar{q}'$ states, a significant natural-parity exchange production of a spin-exotic wave with $J^{PC} = 1^{-+}$ decaying to $\rho\pi$ is found, with an intensity of the resonant part corresponding to $(1.7 \pm 0.2)\%$ of the total intensity in the mass-dependent fit. Its mass-dependent phase differences to the $J^{PC} = 2^{-+}$ and 1^{++} waves are consistent with the highly debated $\pi_1(1600)$ meson.

We gratefully acknowledge the support of the CERN management and staff as well as the skills and efforts of the technicians of the collaborating institutions. This work is supported by MEYS (Czech Republic); BMBF and DFG cluster of excellence "Origin and Structure of the Universe" (Germany); SAIL (CSR) (India); ISF (Israel); INFN (Italy); MEXT, JSPS, Daiko, and Yamada Foundations (Japan); KBN and Ministry of Science and Higher Education (Poland); FCT (Portugal); and CERN-RFBR (Russia).

*Deceased.
†Also at IST, Universidade Técnica de Lisboa, Lisbon, Portugal.
‡On leave from JINR Dubna.
§Also at Chubu University, Kasugai, Aichi, 487-8501 Japan.
‖Also at GSI Helmholtzzentrum für Schwerionenforschung GmbH, D-64291 Darmstadt, Germany.
¶Also at KEK, 1-1 Oho, Tsukuba, Ibaraki, 305-0801 Japan.

[1] K. J. Juge, J. Kuti, and C. Morningstar, AIP Conf. Proc. **688**, 193 (2003).
[2] F. E. Close and P. R. Page, Nucl. Phys. **B443**, 233 (1995).
[3] D. R. Thompson *et al.*, Phys. Rev. Lett. **79**, 1630 (1997).
[4] V. Dorofeev *et al.*, AIP Conf. Proc. **619**, 143 (2002).
[5] A. Abele *et al.*, Phys. Lett. B **423**, 175 (1998).
[6] A. Abele *et al.*, Phys. Lett. B **446**, 349 (1999).
[7] G. S. Adams *et al.*, Phys. Rev. Lett. **81**, 5760 (1998).
[8] S. U. Chung *et al.*, Phys. Rev. D **65**, 072001 (2002).
[9] Y. Khokhlov, Nucl. Phys. **A663–A664**, 596c (2000).
[10] G. M. Beladidze *et al.*, Phys. Lett. B **313**, 276 (1993).
[11] E. I. Ivanov *et al.*, Phys. Rev. Lett. **86**, 3977 (2001).
[12] J. Kuhn *et al.*, Phys. Lett. B **595**, 109 (2004).
[13] D. V. Amelin *et al.*, Phys. At. Nucl. **68**, 359 (2005).
[14] M. Lu *et al.*, Phys. Rev. Lett. **94**, 032002 (2005).
[15] C. A. Baker *et al.*, Phys. Lett. B **563**, 140 (2003).
[16] A. R. Dzierba *et al.*, Phys. Rev. D **73**, 072001 (2006).
[17] P. Abbon *et al.*, Nucl. Instrum. Methods Phys. Res., Sect. A **577**, 455 (2007).
[18] G. Ascoli *et al.*, Phys. Rev. Lett. **25**, 962 (1970).
[19] J. P. Cummings and D. P. Weygand, Brookhaven National Laboratory Report No. BNL-64637 (unpublished).
[20] S. Neubert, http://sourceforge.net/projects/rootpwa.
[21] S. U. Chung and T. L. Trueman, Phys. Rev. D **11**, 633 (1975).
[22] S. U. Chung, Report No. CERN-71-08, in Academic Training Program of CERN, 1969–1970, 1971.
[23] R. T. Deck, Phys. Rev. Lett. **13**, 169 (1964).
[24] C. Daum *et al.*, Nucl. Phys. **B182**, 269 (1981).
[25] W. M. Yao *et al.*, J. Phys. G **33**, 1 (2006).
[26] C. Amsler *et al.*, Phys. Lett. B **667**, 1 (2008).
[27] S. U. Chung and J. Friedrich, Phys. Rev. D **78**, 074027 (2008).